

# Recent developments in the synthesis of FeS<sub>2</sub> nanostructures

Braham Dutt Arya<sup>1</sup>, Priyashree Sindhu<sup>2</sup>

<sup>1,2</sup> Asst. Proff., Dept of Chemistry, Pt. Neki Ram Sharma Govt. College, Rohtak, Haryana, India

## ABSTRACT

Nanomaterial encompass a variety of materials with Nano scale structural features, including nanoparticles, nanofibres and nanocomposites. FeS<sub>2</sub> nanostructures have emerged as a fascinating candidate for their used in various devices such as sensors, superconductors, thermoelectric and drug delivery carriers due to their attractive physical and chemical properties. Generally synthesize in the form of spherical nanoparticles, nanorods, nanowires and nanosheets they have different applications respectively. Depending on their applications they can be synthesized in various shapes, sizes and morphological physical states. During the last few years, there have been a lot of works reported for the phase specific synthesis of FeS<sub>2</sub> nanostructures. To date, despite of the intensive progress in the nanomaterials research and synthesis, only a few attempts to synthesis the single phase or phase specific synthesis of FeS<sub>2</sub> nanostructures have been made. Interestingly, during the last few years a lot of attempts have been made for the synthesis of phase and shape specific synthesis of these nanostructures. Hot injection method, wet chemical method, solvothermal process and chemical vapour deposition method are the latest method being used in this direction. Solvent have a key role to determine the composition as well as the structure of the material formed during its synthesis.

**Key words:** FeS<sub>2</sub> nanostructures; pyrite phase; solvothermal; Hot injection method; wet chemical synthesis

## I. INTRODUCTION

The synthesis of Nano scaled inorganic materials has been a very fascinating field among researchers because of their attractive chemical and physical properties and for their numerous applications in devices, imaging, drug delivery, bio sensing and many more fields. Especially the transition metal chalcogenides shows their potential as thermoelectric, magnetic semiconductors, superconductors, sensors, and photovoltaic. Moreover, Iron chalcogenides have attracted a lot of researchers because of their interesting magnetic, semiconducting, and structural properties. Therefore, they have been targeted for potential use in biomedical applications, including protein immobilization and separation, magnetic targeting and drug delivery, cancer hyperthermia, magnetic resonance imaging (MRI), etc. a lot of available literature about the synthesis of FeS and FeS<sub>2</sub> nanomaterials and their combined use with some other nanomaterials to be target for drug delivery, protein immobilizations and magnetic targeting etc. Fe nanomaterial have shown their usage as single molecular magnets which can provide a new area to the researcher.

The bulk form of pyrite FeS has a band gap energy of 0.95 eV and high optical absorption coefficient of  $5 \times 10^5 \text{ cm}^{-1}$ . Due to these two parameters and their combination with the possibility to vary the band gap using different geometries of nanoscale forms of FeS<sub>2</sub> makes possibility to use them as almost ideal semiconductor for harvesting broad spectrum of light with wavelengths as long as 750 nm. Pyrite can also be a promising material for lithium batteries and is currently used in Energizer batteries. Due to the unique properties along with potentially low costs, environmental friendliness, and ease to form give pyrite a great advantage and scope to attract a number of researcher to study the nanoscale chemistry of FeS<sub>2</sub>.

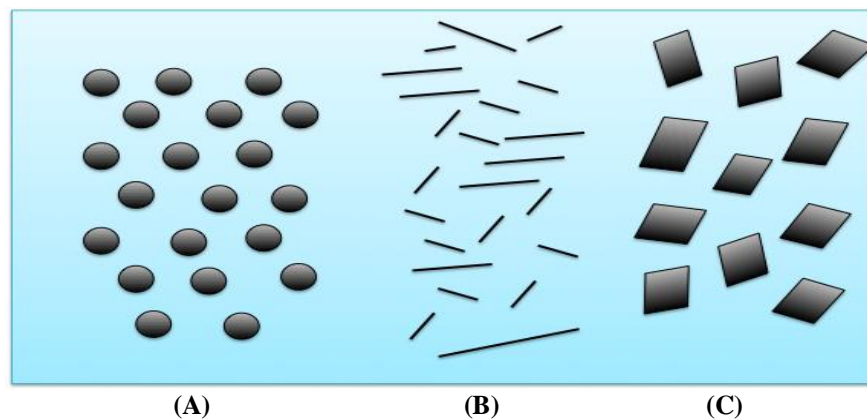
## II. PHYSICAL STATES

FeS<sub>2</sub> exhibits a variety of nanostructures among them spherical nanoparticles (NPs), Nano rods (NRs), Nanowires (NWs) and Nano sheets (NSs) are major. Depending upon the significance they can be used in different forms.

Spherical FeS<sub>2</sub> nanoparticles have shown their numerous applications to be used as a promising candidate for drug delivery with very nominal value of cytotoxicity.

Similarly, nanorods can be used as a potential carrier for protein immobilization and targeted delivery and nanowires and nanosheets shows their promising applications among photovoltaic properties and use in the solar cell. 2D FeS<sub>2</sub> disc nanostructures are an efficient and stable hydrogen evolution electrocatalyst. The 2D FeS<sub>2</sub> disc structure has the highest electro catalytic activity for the hydrogen evolution reaction, comparable to platinum in neutral pH conditions<sup>25</sup>.

The spherical NPs have a lot of applications as zero-dimensional nanoscale semiconductor, one-dimensional nanoscale varieties of FeS<sub>2</sub> such as NRs and NWs. Two-dimensional nanoscale structures, such as NSs, gain even greater importance after many trials and tribulations related to integration of graphene and related materials in electronic and energy storage devices<sup>25</sup>.



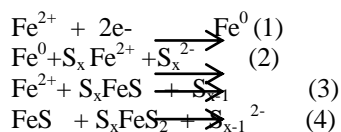
**Schematic 1: Spherical nanoparticles (a); 1D nanorods and nanowires (b) and 2D nanosheets (c)**

## III. METHODS OF SYNTHESIS

Bai et al., 2013 have reported the universal synthesis of single phase pyrite FeS<sub>2</sub> nanoparticles, Nanowires and Nanosheets. According to that report, 0.259 g (1.30 mmol) of FeCl<sub>2</sub>·4H<sub>2</sub>O was dissolved in 90 mL of dimethyl sulfoxide (DMSO) with desired amount of thioglycolic acid (TGA). The solution of the stabilizer was then placed in a three-necked flask fitted with a valve under the N<sub>2</sub> gas atmosphere bubbling of 99.99% nitrogen for 30 min. A solution of Na<sub>2</sub>S<sub>2</sub>O<sub>3</sub>·5H<sub>2</sub>O obtained by the dissolution of 1.45 g (5.85 mmol) of Na<sub>2</sub>S<sub>2</sub>O<sub>3</sub>·5H<sub>2</sub>O (Aldrich) in 10 mL of 18 MΩ deionized water under N<sub>2</sub> atmosphere was drop wise added into the solution while stirring and continuously purging the reaction media with nitrogen for more 30 min. Firstly, nanocolloids formed then they were brought to boiling temperature, where a observation of change of colour from brown to dark black was perceived. The nanocolloids were allowed to grow and crystallize under conditions of continuous reflux at 139 °C for 2–12 h. The diameter of the resulting NPs is majorly determined by the time of reflux.

The synthesis of nanoparticles, nanowires and nanorods is basically controlled by the relative concentration of the different species taking part in the reaction. The FeS<sub>2</sub> NPs were synthesized when the molar ratio of [Fe<sup>2+</sup>]/[S<sub>2</sub>O<sub>3</sub><sup>2-</sup>]/[TGA] was 1:4.5:4. NRs and NWs could be obtained when the molar ratios of [Fe<sup>2+</sup>]/[TGA] were 1:3 and 1:2, respectively. Ethylenediamine (EDA) is used as cosolvent and costabilizer and partial replacement of DMSO with ethylenediamine (EDA) determines the single directional growth to give Nanowires and Nanorods. The molar ratio of [EDA]/[TGA] was 2:1. EDA was added immediately after all the reactants were dissolved in DMSO but before raising the reaction temperature. Upon completion, the NPs and other nanocolloids were separated from the reaction media by centrifugation. The precipitate was washed several times with ethanol and deionized water. The final products were dried in vacuum at 60 °C for 6 h.

Jasion et al. 2015, have reported a different approach for the synthesis of hyper thin iron sulfide nanostructures for which they utilize a solution hot-injection method, analogous to a previously reported iron sulfide synthesis,<sup>26</sup> to create unique hyper thin iron sulfide nanostructures with atomic layer thickness. In the first step of the synthesis, an octadecylamine (ODA) ligand was added to a Fe<sup>2+</sup> solution to start the seeded growth of ~3–5 nm iron nanoparticles. The ODA ligand acts as both a reducing agent for the Fe<sup>2+</sup> (eq 1) and as a capping layer on the subsequent Nano crystal formation. Next, upon injection of sulfur, the iron seed particles oxidize to form Fe<sup>2+</sup> and S<sub>x</sub><sup>2-</sup> moieties (eq 2) and these species form the FeS<sub>2</sub> nanostructures via eqn 3 and 4.



The formation of low dimensional nanostructures can be controlled by adjustments of the initial concentration of the sulfur. They determined that a 1:6 Fe:S ratio yields wires uniformly separated by a tightly packed layer of ligand with a spacing of approximately 2.7 nm. Increasing the Fe:S ratio to 1:24 results in the formation of discs which appear in a stack of thin sheets also separated by a ligand layer.

Yu et al., 2015; reported the synthesis through facile one-step solvothermal process of air-stable and phase-pure pyrite FeS<sub>2</sub> nanostructures through oriented attachment (OA). The major highlights of their work was that the OA kinetics studies and arrangement of FeS<sub>2</sub> primary clusters are closely related to the solvent used in the reaction. Nanocubes of ~150 nm, spheroidal NCs of ~50 nm, and microspheres assembled from nanoparticles can be selectively prepared by OA in different solvents. FeS<sub>2</sub> nanostructures were typically synthesized by using Fe<sub>2</sub>O<sub>3</sub> as iron source, sulfur powder as sulfur source, and 1-octylamine or 1-octanol as solvent in a stainless steel autoclave under solvothermal conditions. The product synthesized with a 1:1 mixture of 1-octylamine and 1-octanol as mixed solvent. The size, shape and morphology of nanostructures has been controlled by the ratio of the solvents used.

Jiang et al., 2015; have reported the use of wet chemistry to synthesize colloidal metal NCs by thermolytic reduction and demonstrated improved the phase purity of metal chalcogenides.<sup>27,28</sup> Injecting iron pentacarbonyl into elemental S dissolved in oleylamine produced pyrite nanoplates of dimensions 150–500 nm and a thickness of about 30 nm, after 4 h at reaction temperatures above 180 °C.<sup>29</sup> Nanocrystals of pyrite ranging in size from a few to hundred nanometers can be synthesized by dissolving a metal salt and elemental sulfur in an alkylamine combined with another ligand or solvent<sup>30-32</sup>. Oleylamine (OAm) is typically used with ligands that bind more strongly in the synthesis of pyrite NCs. Trioctylphosphine oxide (TOPO) combined with oleylamine enabled control of the size of pyrite cubes in the range from 60 to 200 nm<sup>30</sup>. Hexadecanesulfonate yielded cubic NCs with dimensions of 80 nm in OAm. A mixture of oblate and spheroidal pyrite NCs with diameters of 5–20 nm in which the reaction of FeCl<sub>2</sub> and sulfur by using octadecylamine (ODA, CH<sub>3</sub>(CH<sub>17</sub>)NH<sub>2</sub>) as a capping ligand.<sup>33</sup>

E'jazi et al., 2011 ; synthesis FeS<sub>2</sub> nanoparticles by solvothermal process the major drawback in the previously used methods is the high temperature requirement and additional sulfur usage to convert other phases such as FeS or FeS<sub>2-x</sub> into pyrite<sup>34</sup>. They have used the stainless steel stirred reactor; while in previous studies a stainless-steel cylindrical chamber was used to produce pyrite has been already reported<sup>35-37</sup>. They have used impeller to increase the mass transfer and reported the reduction of the reaction time from 12 to 5 h. They have carried out the experiment in 2000 ml stainless-steel stirred reactor equipped with a temperature controller, a barometer and an axial impeller with four blades, at stirring speed 1000 rpm. In the process reported, an appropriate amount of iron source and sulfur source were mixed with 600 ml of solvent and the mixture was taken into the reactor maintained at desired temperature. The reactor was cooled down to the room temperature (24°C) after 5 h and resulted black precipitates were filtered off and washed sequentially with distilled water and to remove impurities (sulfur) they have carried out washing with CS<sub>2</sub> and finally products were dried at 60 °C for 4 h to get black powder. They reported a range of solvents and a different ratio of the solvents with different raw material as a Fe source, according to that they reported the formation of the different forms of final product whether it is hematite, pyrite or any other form.

**Table1 Fe<sub>2</sub>S<sub>3</sub> Based Nanomaterial Synthesis, Method Used and Different Precursors**

Method	Fe precursors	S precursors	Solvent / stabilizer	Instrument or process	Reference
Universal synthesis (NPs, NRs, NWs)	FeCl <sub>2</sub> .4H <sub>2</sub> O	Na <sub>2</sub> S <sub>2</sub> O <sub>3</sub> .5H <sub>2</sub> O	DMSO/TGA	Reflux	Bai et al., 2013
Hot injection method (hyper thin NSs)	FeCl <sub>2</sub> .4H <sub>2</sub> O	Sulfur Powder	octadecylamine	Reflux and stirring	Jasion et. al.,2015
Solvothermal process (NCs)	Fe <sub>2</sub> O <sub>3</sub>	Sulfur powder	1-octylamine & 1-octanol	Oriented attachment	Yu et. al, 2015
Wet chemistry synthesis(NPs,NCs)	Fe(CO) <sub>5</sub>	Elemental sulfur	oleylamine & Trioctylphosphine oxide	Thermolytic reduction	Jiang et. al, 2015
Solvothermal process(NPs)	FeSO <sub>4</sub> .7H <sub>2</sub> O	NH <sub>2</sub> CSNH <sub>2</sub> Na <sub>2</sub> S <sub>2</sub> O <sub>3</sub> .5H <sub>2</sub> O	Ehtylenediamine, ethanol, 1-butanol	Stainless steel reactor	E'jazi et. al., 2011
Chemical vapor deposition (thin films)	FeCl <sub>3</sub>	Ditertbutylsulfide (TBDS)	Inert atmosphere (argon)	CVD system	Samad et. al,2015

Samad et al., 2015; have reported the direct chemical vapor deposition synthesis of phase-pure Iron Pyrite (FeS<sub>2</sub>) thin films. Using Ditert butyl disulfide (TBDS) and FeCl<sub>3</sub> as the sulfur and iron precursors, respectively. The TBDS precursor was loaded into a glass bubbler and connected to a custom-built CVD system using stainless steel tubing, a silica reaction tube in a Lindberg Blue tube furnace, which was connected to a vacuum pump, and gas flow controllers followed by the addition of the FeCl<sub>3</sub> powder in an alumina boat in an inert atmosphere glovebox and transferred in a sealed vial to prevent water uptake. The FeCl<sub>3</sub> was placed in the 300 °C temperature zone of the furnace, and the TBDS bubbler was submerged in an oil bath at 85 °C, resulting in a vapor pressure of ~280 Torr for the sulfur and FeCl<sub>3</sub>. The CoS<sub>2</sub> substrates were placed in the 400–425 °C temperature range of the furnace. They have reported the time span of the reaction is 1–4 h under a pressure of 760 Torr with a total argon flow rate of 250 sccm split through the TBDS bubbler and over the FeCl<sub>3</sub> precursor.

### CONCLUSION AND FUTURE PROSPECTS

It was concluded that synthesis of nanomaterial is basically physical as well as chemical conditions dependent. Effect of temperature, time span of the reaction, nature of the solvent used and the interaction of the solvent with the starting material plays an important role and that's why these all collectively determine the shape, size and morphology of the material. Different kind of methods has diverse use different precursors and different approach to synthesize different nanostructures. Size, shape dependent synthesis is the major deciding parameter. Presence of inert atmosphere is also the necessary requirement for obtaining the desired nanomaterial. The major problem among us is the aerial oxidation of the synthesized product. We need to demonstrate some method in which we can produce the FeS<sub>2</sub> nanostructures without oxidizing them. Washing is the most crucial step, because here are the maximum chances of oxidation. So synthesis parameters should be maintain in such a way aerial oxidation can be minimized. FeS<sub>2</sub> nanostructures have wide applications. There use as drug delivery carriers is also the field of very high interest. They have a major scope in the field of drug delivery. Photovoltaics, superconductor devices, bio sensing and bio imaging all fields require improved methods for the synthesis of these nanostructures with improved qualities. just like other transition metal chalcogenides FeS<sub>2</sub> nanostructures have a wide scope in the today material synthesis. They can show wide applications with the Graphene Oxide(wonder material) based nanocomposites, that need more to be explore.

### REFERNECES

- [1] Sardar, K. and Rao, C. N. R. (2004), New Solvothermal Routes for GaN Nanocrystals. Adv. Mater., 16: 425–429.
- [2] Rao, C. N. R.; Deepak, F. L.; Gundiah, G.; Govindaraj, Inorganic nanowires Progress in Solid State Chem. 2003, 31, 5.
- [3] J.T. Hu, T.W. Odom, C.M. Lieber, 1999, Chemistry and physics in one dimension: synthesis and properties of nanowires and nanotubes, Acc. Chem. Res. 32 (5), 435-445.
- [4] Wood, C.; Materials for thermoelectric energy conversion; Rep. Prog. Phys. 1988, 51 (4), 459.
- [5] Dietl, T.; Ferromagnetic semiconductors; Semicond. Sci. Technol. 2002, 17 (4), 377
- [6] Niu, H. J.; Hampshire, D. P. Critical parameters of disordered nanocrystalline superconducting Chevrel-phase
- [7] PbMo<sub>6</sub>S<sub>8</sub>; Phys. Rev. B 2004, 69 (17), 174503.
- [8] Schoning, M. J.; Kloock, J. P About 20 Years of Silicon-Based Thin Film Sensors with Chalcogenide Glass Materials for Heavy Metal Analysis: Technological Aspects of Fabrication and Miniaturization- A review . Electroanalysis 2007, 19 (19–20), 2029.

- [9] Ennaoui, A.; Fiechter, S.; Pettenkofer, C.; Alonsovante, N.; Buker, K.; Bronold, M.; Hopfner, C.; Tributsch, H.; Iron disulfide for solar energy conversion; *Sol. Energy Mater. Sol. Cells* 1993, 29 (4), 289.
- [10] Huynh, W. U.; Dittmer, J. J.; Alivisatos, A. P.; Hybrid nanorod-polymer solar cells; *Science* 2002, 295 (5564), 2425.
- [11] Mitzi, D. B.; Yuan, M.; Liu, W.; Kellock, A. J.; Chey, S. J.; Deline, V.; Schrott, A. G.; A High-Efficiency Solution-Deposited Thin-Film Photovoltaic Device; *Adv. Mater.* 2008, 20 (19), 3657.
- [12] Bonneau, P. R.; Jarris, R. R., Jr.; Kaner, R. B. Rapid solid-state synthesis of materials from molybdenum disulphide to refractories; *Nature* 1991, 349, 510.
- [13] Ferrer, I. J.; Caballero, F.; Delas, H. C.; Sarchez, C.; Preparation of n type doped FeS<sub>2</sub> thin films; *Solid State Commun.* 1994, 89, 349.
- [14] Tang, K. B.; Qian, Y. T.; Zeng, J. H.; Yang, X. G. Solvothermal route to semiconductor nanowires; *Adv. Mater.* 2003, 15, 448. Perez, J. M.; Simeone, F. J.; Tsourkas, A.; Josephson, L.; Weissleder, R. Peroxidase substrate nanosensors for MR imaging *Nano Lett.* 2004, 4, 119. (b) Oscar, B. M.; Maria, P. M.; Pedro, T.; Jesus, R. C.; Pierre, B.; Martin, S.; Zhao, X. Q.; Sabino, V. V. Fe-based nanoparticulate metallic alloys as contrast agents for magnetic resonance imaging *Biomaterials* 2005, 26, 5695.
- [15] Cheng, J. J.; Teply, B. A.; Jeong, S. Y.; Yim, C. H.; Ho, D.; Sherifi, I.; Jon, S.; Farokhzad, O. C.; Khademhosseini, A. R.; Langer, Magnetically responsive polymeric microparticles for oral delivery of protein drugs *S. Pharm. Res.* 2006, 23, 557.
- [16] Yang, Y.; Jiang, J. S.; Du, B.; Gan, Z. F.; Qian, M.; Zhang, P. Preparation and properties of a novel drug delivery system with both magnetic and biomolecular targeting *J. Mater. Sci.: Mater. Med.* 2009, 20, 301.
- [17] Gou, M. L.; Qian, Z. Y.; Wang, H.; Tang, Y. B.; Huang, M. J.; Kan, B.; Wen, Y. J.; Dai, M.; Li, X. Y.; Gong, C. Y.; Tu, M. J. J. Preparation and characterization of magnetic poly(epsilon-caprolactone)-poly(ethylene glycol)-poly(epsilon-caprolactone) microspheres *Mater. Sci.: Mater. Med.* 2008, 19, 1033.
- [18] (a) Matteucci, M. L.; Anyarambhatla, G.; Rosner, G.; Azuma, C.; Fisher, P. E.; Dewhirst, M. W.; Needham, D.; Thrall, D. E. Hyperthermia increases accumulation of technetium-99m-labeled liposomes in feline sarcomas *Clin. Cancer Res.* 2000, 6, 3748. (b) Majoros, I. J.; Myc, A.; Thomas, T.; Mehta, C. B.; Baker, J. R. PAMAM dendrimer-based multifunctional conjugate for cancer therapy: synthesis, characterization, and functionality. *Biomacromolecules* 2006, 7, 572.
- [19] Braehler, M.; Georgieva, R.; Buske, N.; Muller, A.; Muller, S.; Pinkernelle, J.; Teichgraber, U.; Voigt, A.; Banmler, H. Magnetite-loaded carrier erythrocytes as contrast agents for magnetic resonance imaging *Nano Lett.* 2006, 6, 2505.
- [20] Denis, M. C.; Mahmood, U.; Benoist, C.; Mathis, D.; Weissleder, Imaging inflammation of the pancreatic islets in type 1 diabetes *R. Proc. Natl. Acad. Sci. U. S. A.* 2004, 101, 12634.
- [21] Bulte, J. W. Intracellular endosomal magnetic labeling of cells *Methods Mol. Med.* 2006, 124, 419.
- [22] Ennaoui, A.; Fiechter, S.; Jaegermann, W.; Tributsch, H. J. Energetic characterization of the photoactive FeS<sub>2</sub> (pyrite) interface. *Sol Energy Mater Electrochem. Soc.* 1986, 133, 97–106.
- [23] Ennaoui A, Fiechter S, Pettenkofer C, Alonso-Vante N, Bükler K, Bronold M, Höpfner C and Tributsch H 1993 Iron disulfide for solar energy conversion *Sol. Energy Mater. Sol. Cells* 29 289–370.
- [24] Feng, X.; He, X. M.; Pu, W. H.; Jiang, C. Y.; Wan, Synthesis of nanosized Si composite anode material for Li-ion batteries *C. R. Ionics* 2007, 13, 375–377.
- [25] Daniel Jasion, Joseph M. Barforoush, Qiao Qiao, Yimei Zhu, Shenqiang Ren, and Kevin C. Leonard Low-Dimensional Hyperthin FeS<sub>2</sub> Nanostructures for Efficient and Stable Hydrogen Evolution Electrocatalysis; *ACS Catal.* 2015, 5, 6653–6657
- [26] Rosso, K. M.; Becker, U.; Hochella, M. F. Atomically resolved electronic structure of pyrite {100} surfaces: An experimental and theoretical investigation with implications for reactivity *Am. Mineral.* 1999, 84, 1535–1548.
- [27] Talapin, D. V.; Rogach, A. L.; Shevchenko, E. V.; Kornowski, A.; Haase, M.; Weller, H. Dynamic Distribution of Growth Rates within the Ensembles of Colloidal II-VI and III-V Semiconductor Nanocrystals as a Factor Governing Their Photoluminescence Efficiency. *J. Am. Chem. Soc.* 2002, 124, 5782–5790.
- [28] Shieh, F.; Saunders, A. E.; Korgel, B. A. General Shape Control of Colloidal CdS, CdSe, CdTe Quantum Rods and Quantum Rod Heterostructures. *J. Phys. Chem. B* 2005, 109, 8538–8542.
- [29] Kirkemünde, A.; Ruzicka, B. A.; Wang, R.; Puna, S.; Zhao, H.; Ren, S. Synthesis and Optoelectronic Properties of Two-Dimensional FeS<sub>2</sub> Nanoplates. *ACS Appl. Mater. Interfaces* 2012, 4, 1174–1177.
- [30] Bi, Y.; Yuan, Y.; Exstrom, C. L.; Darveau, S. A.; Huang, J. Air Stable, Photosensitive, Phase Pure Iron Pyrite Nanocrystal Thin Films for Photovoltaic Application. *Nano Lett.* 2011, 11, 4953–4957.
- [31] Puthussery, J.; Seefeld, S.; Berry, N.; Gibbs, M.; Law, M. Colloidal Iron Pyrite (FeS<sub>2</sub>) Nanocrystal Inks for Thin-Film Photovoltaics. *J. Am. Chem. Soc.* 2011, 133, 716–719.
- [32] Steinhagen, C.; Harvey, T. B.; Stolle, C. J.; Harris, J.; Korgel, B. A. Pyrite Nanocrystal Solar Cells: Promising, or Fool's Gold? *J. Phys. Chem. Lett.* 2012, 3, 2352–2356.
- [33] Thomson, J. W.; Nagashima, K.; Macdonald, P. M.; Ozin, G. A. From Sulfur-Amine Solutions to Metal Sulfide Nanocrystals: Peering into the Oleylamine-Sulfur Black Box. *J. Am. Chem. Soc.* 2011, 133, 5036–5041
- [34] R. Wu, Y.F. Zheng, X.G. Zhang, Y.F. Sun, J.B. Xu, J.K. Jian, Hydrothermal synthesis and crystal structure of pyrite, *J. Cryst. Growth* 266 (2004) 523–527.
- [35] Q. Xuefeng, X. Yi, Q. Yitai, Solventothermal synthesis and morphological control of nanocrystalline FeS<sub>2</sub>, *Mater. Lett.* 48 (2001) 109–111.
- [36] S. Kar, S. Chaudhuri, Solventothermal synthesis and morphological control of nanocrystalline FeS<sub>2</sub>, *Chem. Phys. Lett.* 398 (2004) 22–26.
- [37] Soumitra Kar, Subhadra Chaudhuri, Synthesis of highly oriented iron sulfide nanowires through solvothermal process, *Mater. Lett.* 59 (2005) 289–292.